



Journal of Applied Sciences

ISSN 1812-5654

science
alert

ANSI*net*
an open access publisher
<http://ansinet.com>

Effect of the Moments of Probability Density Function for Non-uniform Air Flow Distribution on the Hydraulic Performance of a Fin-tube Heat Exchanger

Wai Meng Chin and Vijay R. Raghavan

Department of Mechanical Engineering, Universiti Teknologi PETRONAS,
Bandar Seri Iskandar, 31750 Tronoh, Perak, Malaysia

Abstract: The work presented in this paper examines the effect of a non-uniform airflow velocity distribution on the air pressure drop through the fin passages of a single row fin-tube heat exchanger. Water flow rate through the tubes and its temperature are taken as constant. Maldistribution of the airflow increases the average pressure drop with respect to that of a uniform flow. As a result of this, the pumping power required by the fan or blower will also increase. The increase of the pumping power is calculated by means of a discretization technique and it is analyzed with respect to the non-uniform distribution statistical moments of probability density function, i.e., the mean, standard deviation, skew and kurtosis. The analysis reveals that the increase of pumping power is dependent on the exchanger NTU, standard deviation and skew of the velocity distribution. Kurtosis has no effect on the pressure drop. Correlations have been developed to predict this increase of pumping power from known statistical moments and resulting air temperatures. These can then be used as design tools to optimize the sizing of the heat exchanger within the air-conditioning unit, hence giving the best energy efficiency performance.

Key words: Maldistribution, pumping power, standard deviation, skew, kurtosis

INTRODUCTION

Air-conditioning systems have become a necessity in almost all types of buildings. A study (U.S. Energy Information Administration, 2009) has shown that Malaysia consumed approximately 96 billion kWh of electrical energy in 2006, where well over one-third was used in commercial buildings (Zain-Ahmed, 2008). It was also estimated that approximately 50% of the energy used in buildings was due to the installed HVAC systems (Perez-Lombard *et al.*, 2008). Consequently, any effort to improve the energy efficiency of air-conditioning systems will contribute significantly to energy savings.

Fin-tube heat exchangers, more commonly called coils, are used extensively in air-conditioning units. They are used primarily as evaporators and condensers in the system. These coils have stacked aluminum fins which are held together by copper tubes inserted through holes punched on the fin surface. Air flows over the fin surfaces through the multiple passages created by the fins, while a refrigerant flows in the tubes.

In most designs, the heat exchanger is sized by assuming uniform distribution for both fluid streams. However, such uniformity does not occur in practice. Maldistribution of both fluids will take place as a result of the mechanical disposition of the air-conditioning unit.

The unit design and location of the coil with respect to the other components in the unit will affect the distribution profile of air in the exchanger.

It is known that Maldistribution affects the performance of heat exchangers. Not only does the fluid pressure drop increase but the heat transfer performance also reduces. The increase in pressure drop will then result in a higher pumping power for the fan or blower.

Hence, prior knowledge of the Maldistribution profile is beneficial to the designer in arriving at an optimum size for a given duty. The design layout of the unit could be changed to give a more favorable air distribution to the exchanger. It is imperative that the negative effects of Maldistribution are minimized which thus enables the exchanger to operate with higher levels of energy efficiency.

STATISTICAL MOMENTS

The profile of a Maldistribution can be characterized by its four statistical moments of mean, standard deviation, skew and kurtosis. If all four moments are equal between two distributions, both distributions can be assumed to have similar characteristics, though not necessarily having the same profile shape.

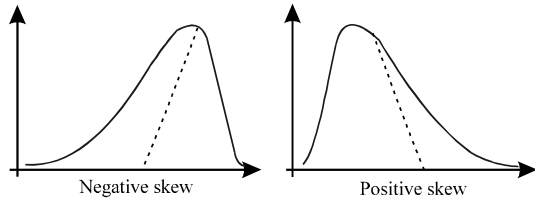


Fig. 1: Illustration of distribution skew

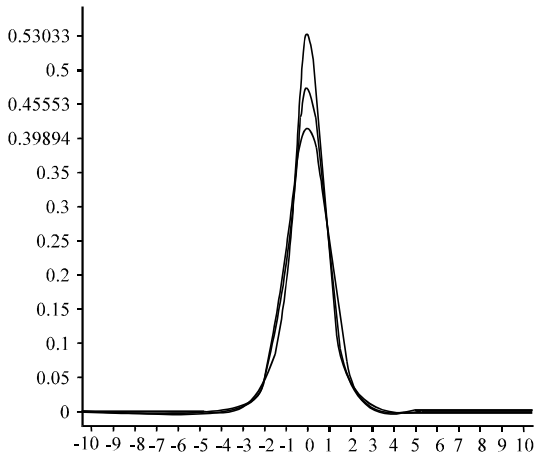


Fig. 2: Example of a distribution with kurtosis of infinity (top), 2 (center) and 0 (bottom) (<http://en.wikipedia.org/wiki/Kurtosis>)

The first moment of a probability density function, which is the mean (μ), gives the average value of the distribution. The second moment, i.e. standard deviation (σ) defines the variability or dispersion of the distribution.

The third moment, skew (γ) is a measure of the lop-sidedness of the distribution. A distribution with positive skew will have an elongated tail to the right; and vice-versa. This is illustrated in Fig. 1.

The fourth moment is a measure of how tall and slender or short and squat a distribution is when compared with a normal distribution. Positive kurtosis indicates a relatively peaked distribution while a negative value corresponds to a flat distribution, as can be seen from Fig. 2.

In this work, the mean, standard deviation, skew and kurtosis, for a sample size of n , are calculated by using the following sample unbiased estimator equations:

- **Sample mean \bar{x} :**

$$\bar{x} = \frac{\sum_{i=1}^n x_i}{n} \quad (1)$$

- **Sample standard deviation (s):**

$$s^2 = \frac{\sum_{i=1}^n (x_i - \bar{x})^2}{(n-1)} \quad (2)$$

- **Sample skew (g_1):**

$$g_1 = \frac{n}{(n-1)(n-2)} \sum_{i=1}^n \left(\frac{x_i - \bar{x}}{s} \right)^3 \quad (3)$$

- **Sample kurtosis (g_2):**

$$g_2 = \frac{n(n+1)}{(n-1)(n-2)(n-3)} \sum_{i=1}^n \left(\frac{x_i - \bar{x}}{s} \right)^4 - \frac{3(n-1)^2}{(n-2)(n-3)} \quad (4)$$

MATERIALS AND METHODS

An analytical model of the fin-tube heat exchanger is used to simulate the thermal and air pressure drop performance with different profiles of air velocity Maldistribution. For this model, a single row heat exchanger coil was used. The coil has 10 tubes, with 9.52 mm outer diameter, where hot water flows in each parallel tube through the fins. The tube pitch is 25.4 mm. The coil also has wavy corrugated fins with a fin pitch of 1.411 mm. The coil length is 600 mm.

The entire coil face area is discretized into 100 elements, as shown in Fig. 3. Each element is treated as an individual cross-flow heat exchanger. By assigning individual velocity values for each discrete coil element, the velocity maldistribution profile over the entire coil is established.

By manipulating various forms of known probability density functions, e.g., the Normal distribution, the moments of the velocity maldistribution are varied within the following ranges:

- Standard deviation: 0.10 to 0.80
- Skew: -1.08 to +1.08
- Kurtosis: -1.00 to +1.00

The air volume flow rate through the coil is varied between 0.06 and 0.4 $m^3 \text{ sec}^{-1}$. The water temperature in the tube is systematically varied from 40 to 70°C while the inlet air temperature ranged from 15 to 45°C. At the

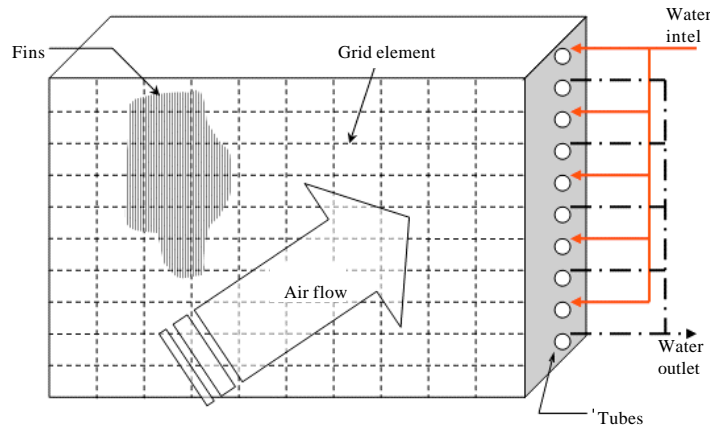


Fig. 3: Schematic diagram of heat exchanger model

same time, the assumed internal heat transfer coefficient is also systematically changed from 4,540 to 147,600 W/m²K, which corresponds to fully turbulent flow in the tubes, i.e. with Re > 10,000.

For each discrete element, the air pressure drop, ΔP, is calculated from the following equation (Kays and London, 1984);

$$\Delta P = \frac{G^2 v_i}{2g} \left[(1 + \vartheta^2) \left(\frac{v_o}{v_i} - 1 \right) + f \left(\frac{A_o}{A_c} \right) \left(\frac{v_m}{v_i} \right) \right] \quad (5)$$

where, G is air mass flux, A_o and A_c are the total external area and fin passage cross-section area respectively, v_m, v_o and v_i are the mean, outlet and inlet air specific volumes respectively, ϑ is the ratio of the fin minimum free-flow area to the coil frontal area, and f is the friction factor.

However, calculation of Eq. 5 will require the air outlet temperature to be known. Therefore, the heating capacity of each element must be known first. To do this, the overall heat transfer coefficient for each discrete element, U_o, is determined from the thermal resistance equation, as;

$$\frac{1}{U_o A_o} = \frac{1}{\eta_s h_o A_o} + \frac{\ln(D_o/D_i)}{2\pi k_c L A_o} + \frac{1}{h_i A_i} \quad (6)$$

where, A_i is the total internal surface areas, D_o and D_i are the tube external and internal diameters respectively, h_o and h_i are the external and internal heat transfer coefficients, η_s is the fin surface efficiency, L is the tube length and k_c is the tube wall thermal conductivity.

In Eq. 5 and 6, the friction factor, f, and the external heat transfer coefficient, h_o, are calculated from the

correlations developed by Wang *et al.* (1999) for wavy corrugated fin pattern. The internal heat transfer correlation is obtained from the well-known Dittus-Boelter equation. With these, U_o is calculated for each coil element and the elemental heat transfer (Q_i) is determined from;

$$Q_i = \epsilon C_{\min} (T_{w,i} - T_{a,i}) \quad (7)$$

where, T_{w,i} and T_{a,i} are the water and air entering temperatures respectively, C_{min} is the minimum heat capacity rate and ε is the heat exchanger effectiveness. ε is a function of the number of thermal units, NTU, where:

$$NTU = U_o A_o / C_{\min} \quad (8)$$

and:

$$\epsilon = \frac{1}{C_r} (1 - \exp[-C_r (1 - \exp(NTU))]) \quad (9)$$

where, C_r is the ratio of the minimum to maximum fluid heat capacity rates. With Q_i known, the air temperature leaving the element can be determined, thus enabling the air exit specific volume to be calculated for Eq. 5.

The heat exchanger NTU is then calculated from each of the discrete elements from:

$$NTU = \frac{\sum_i U_{o,i} A_{o,i}}{\sum_i C_{\min,i}} \quad (10)$$

RESULTS AND DISCUSSION

All the required equations for each element have been assembled into a Microsoft EXCEL spreadsheet with Visual Basic macro programming to calculate the elemental air pressure drop and heating capacity. For ease of handling, all the elemental velocities are normalized by dividing with the average coil face velocity.

There are two possible ways to quantify the degree of increase in pressure drop of the coil, i.e., by calculating:

- Mass-average pressure drop ($\Delta p_{m,avg}$)
- Pumping power (P_w)

The first one is defined for all the elements, i , as:

$$\Delta p_{m,avg} = \frac{\sum_i m_i \Delta p_i}{\sum_i m_i} \tag{11}$$

where, m_i is the elemental air mass flow rate; while the second parameter is defined as:

$$P_w = \sum_i q_i \Delta p_i \tag{12}$$

where, q_i is the elemental air volume flow rate. Essentially, both of these parameters are similar.

In this work, the second parameter is selected. This is because the pumping power can be measured during experimentation for validation. The effect due to the maldistribution is then quantified by using the pumping power penalty factor (P_p) defined as:

$$P_p = \frac{P_{w,maldistribution} - P_{w,uniform}}{P_{w,uniform}} \times 100\% \tag{13}$$

The analysis was firstly carried out to examine the effects of the kurtosis. For this, a set of maldistribution profiles with standard deviation = 0.35 and skew = 0.00 was used to calculate the pumping power. The results of the calculation also show that the kurtosis does not exert a significant effect on the air pumping power of the heat exchanger. This can be seen from Fig. 4 where the pumping power exhibits a flat trend line with respect to the kurtosis.

Consequently, the magnitude of kurtosis was not controlled when generating the maldistribution profiles with the other three moments.

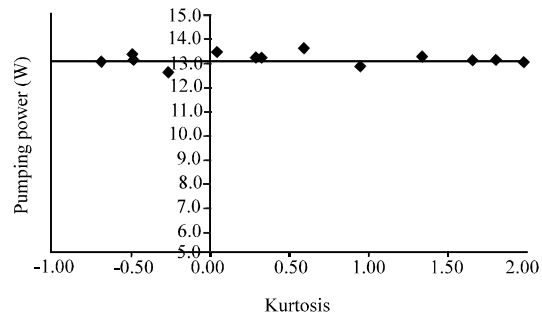


Fig. 4: Trend of pumping power vs. kurtosis (Standard deviation = 0.35, skew = 0.0)

The results of the increase in pumping power can then be presented in a P_p -NTU plot, as seen in the example shown in Fig. 5 for a specific skew and h_c .

Higher NTU corresponds to lower air mass flow rates (i.e., lower C_{min}). Evidently, the reduction in air velocity causes the increase of air pumping power to drop. The air pressure drop penalty becomes higher as the air velocity increases. This corresponds to the known relationship where the pressure drop, ΔP , varies as the air face velocity, V_f raised to the power of n , where $n > 1$;

$$\Delta P = k V_f^n \tag{14}$$

The trend of the line shows that P_p varies as the square of NTU. Higher standard deviation causes P_p to increase. The plots of Fig. 5 also show that at low standard deviations, e.g. at 0.104, the changes of P_p become insignificant.

The data can also be re-plotted, at a specific NTU value, and at a specific h_c , to give the relationship between P_p and standard deviation. This is shown in Fig. 6. It is observed that P_p varies as the square or cube of standard deviation. Also, as the maldistribution skew decreases, the increase of pumping power reduces. This corresponds to the larger proportion of velocity in the distribution having lower velocities. Furthermore, at low standard deviations, the effect of skew is also not significant.

Similarly, the results are re-plotted at a specific NTU value and at a specific h_c , to show the relationship between P_p and skew. This is illustrated in Fig. 7.

The result show that skews has a significant effect on the pumping power, especially at high standard deviations. Skew has no significant effect when the standard deviation is 0.25 or lower. With higher standard deviations (>0.30), the performance varies linearly or as a square of skew. At higher positive skews, the pumping power becomes higher. This is because the distribution has a lot higher velocities, which increase the exchanger

core friction. Conversely, distributions with negative skews show lower pumping power due to the larger proportion of low velocities.

The data is then analyzed to determine the effect of the internal heat transfer coefficient. By plotting the data together for different levels of h_i , at specific skew,

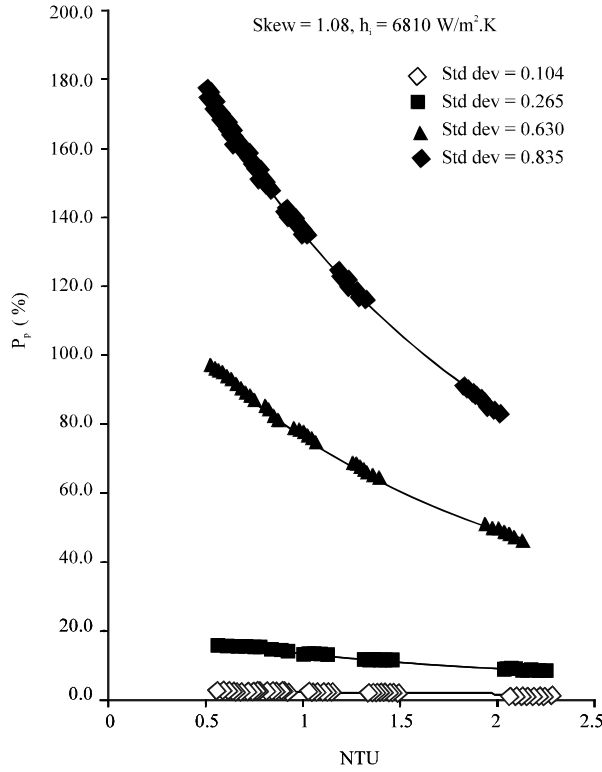


Fig. 5: P_p -NTU plot

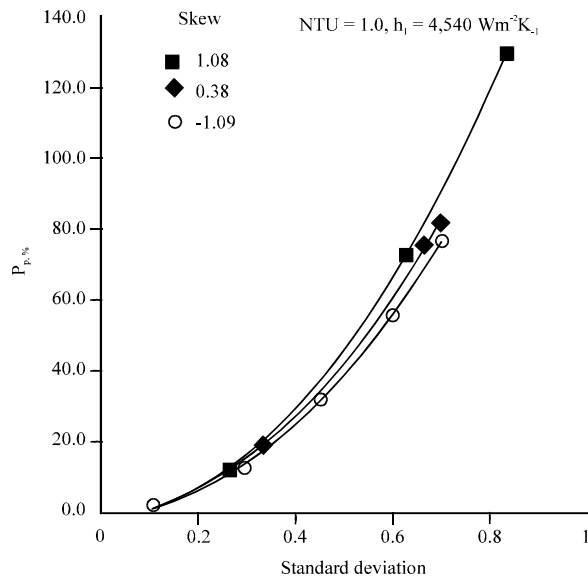


Fig. 6: Trend of pumping power penalty, P_p , with standard deviation

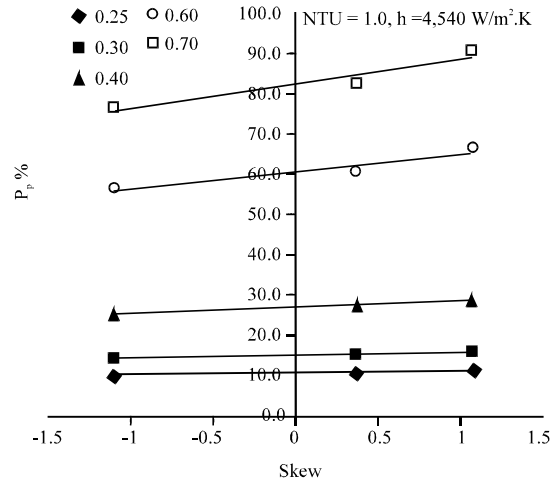


Fig. 7: Trend of pumping power penalty, P_p , with skew

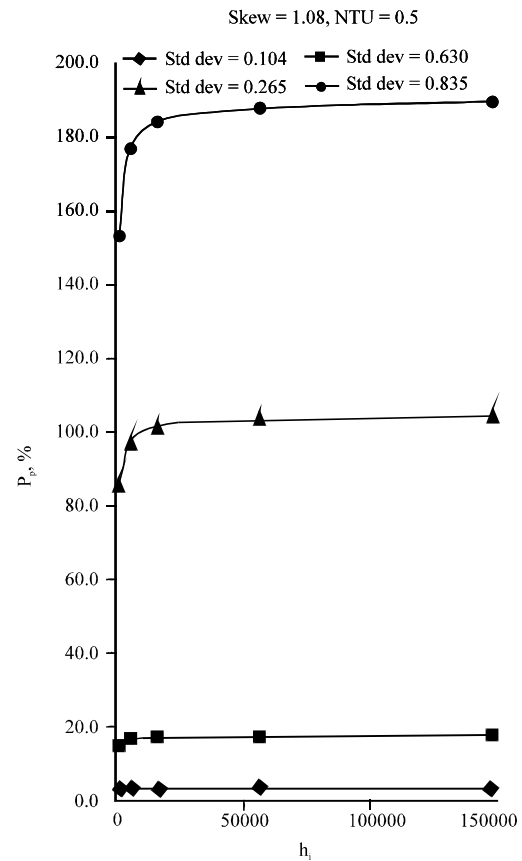


Fig. 8: Trend of pumping power penalty, P_p , with internal heat transfer coefficient, h_i

Table 1: Regression constants

Constant	Values	Constants	Values
a	0.0679	k	-12.414
b	1.707	l	0.898
c	0.011	m	0.159
d	0.242	n	-0.238
e	0.189	o	-109.202
f	1.279	p	0.121
g	-0.037	q	-198.421
h	-0.616	r	-0.402
I	1.370	s	0.511
j	583.461	t	-389.248

standard deviation and NTU, one would get trends as shown in Fig. 8.

As h_i increases, P_p increases. The physical explanation for this is related to the effect of h_i to the thermal performance degradation. It is known that h_i has a reciprocal relationship with the maldistribution thermal degradation effect. Consequently, as h_i increases, the air leaving temperature increases, which increases the air mean specific volume (or reducing the density), hence increasing the pressure drop. Nevertheless, the increase of P_p becomes insignificant when $h_i > 60,000 \text{ W m}^{-2} \cdot \text{K}$.

Correlation Development: With all the obtained data, it is possible to develop a correlation equation to relate the pumping power penalty, P_p , with respect to NTU, standard deviation, σ , and skew, γ . The NTU will account for the changes in mean from the variation of the air flow rate. It will also account for the variation of h_i . Other than that, another parameter, R , which is the ratio of external to internal heat transfer coefficients, is used to correlate the data.

$$R = \frac{h_o}{h_i} \tag{15}$$

From the observed trends of the effects from the statistical moments, the form of the correlation equation is proposed to be as follows:

$$P_p = \left(a\sigma^3 + b\sigma^2 + c\sigma \right) \left(d\gamma^2 + e\gamma + f \right) \left(gN^2 + hN + i \right) \left(jR^2 + kR + l \right) + \sigma^2 \left(m\gamma^2 + nN^2 + oR^2 + p\gamma^2 N^2 + q\gamma^2 R^2 \right) + \sigma^2 \left(r\gamma^2 + sN^2 + tR^2 \right) \tag{16}$$

In the equation above, a, b, c, ..., ..., t are constants, which can be solved by using non-linear regression analysis. For this purpose, the Datafit software (version 9.0) was used. The results of the regression are given in Table 1.

A parity plot of the values predicted from this correlation can then be made with respect to the prior

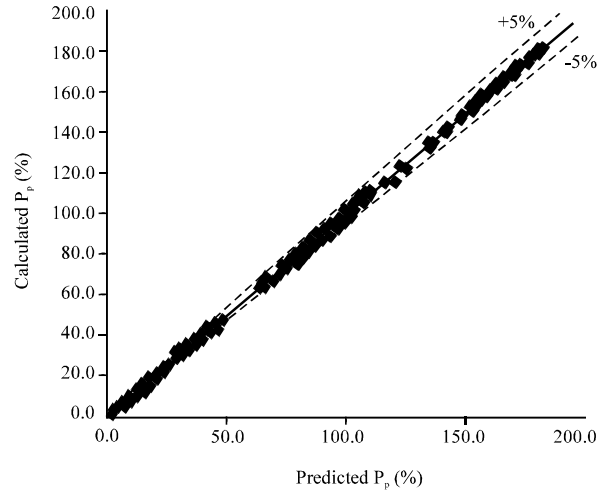


Fig. 9: Parity plot of P_p correlation

calculated values of P_p . The result of this plot is shown in Fig. 9. A good agreement within $\pm 5\%$, between the predicted values using (16) and the calculated values, is obtained within the range of standard deviation from 0.10 to 0.80.

CONCLUSION

Non-uniform distribution of air flow over a fin-tube heat exchanger will increase the core pressure drop. No known prior research has been done to correlate the effects of the four statistical moments on this pressure drop. The pumping power was selected as a criterion to characterize the effects of this maldistribution. The magnitude of hydraulic performance degradation is quantified with the pumping power penalty, P_p .

Of the four statistical moments, only kurtosis does not have any significant effect on P_p . The analysis reveals that:

- P_p varies as the cube of standard deviation
- P_p varies as the square of skew
- P_p varies as the square of NTU
- P_p varies as the square of R

A correlation equation has been developed to predict the magnitude of P_p . The correlation has a good agreement of $\pm 5\%$. With this equation, it is possible to optimize the layout design of an air-conditioning unit to give the lowest possible air pressure drop through the fin-tube heat exchanger; which can therefore reduce the energy consumption of the fan or blower. Maldistribution profiles with low standard deviation and low skew are preferred to give lower hydraulic performance losses.

ACKNOWLEDGMENTS

The authors would like to thank Universiti Teknologi Petronas and O.Y.L. Research and Development Center Sdn. Bhd., Sg. Buloh, Malaysia for their support for this research project.

REFERENCES

- Kays, W.M. and A.L. London, 1984. Compact Heat Exchangers. 3rd Edn., McGraw-Hill, New York, pp: 115-140.
- Perez-Lombard, L., J. Ortiz and C. Pout, 2008. A review on buildings energy consumption information. *Energy Buildings*, 40: 394-398.
- U.S. Energy Information Administration, 2009. Country Analysis Briefs: Malaysia. Independent Statistics and Analysis, September 2009, <http://www.eia.doe.gov/cabs/Malaysia/Background.html>.
- Wang, C.C., J.Y. Jang and N.F. Chiou, 1999. A heat transfer and friction correlation for wavy fin and tube heat exchangers. *Int. J. Heat Mass Transfer*, 42: 1919-1924.
- Zain-Ahmed, A., 2008. Contemporary issues in energy and buildings in Malaysia: Focus on R and D and policies. *SENVAR+IAESE 2008: Humanity and Technology*, pp: 15-23.